



HAL
open science

A single base pair duplication in SLC33A1 gene causes fetal losses and neonatal lethality in Manech Tête Rousse dairy sheep

Maxime Ben Braiek, Soline Szymczak, Céline André, Philippe Bardou, Francis Fidelle, Itsasne Granado-Tajada, Florence Plisson-Petit, Julien Sarry, Florent Woloszyn, Carole Moreno-Romieux, et al.

► To cite this version:

Maxime Ben Braiek, Soline Szymczak, Céline André, Philippe Bardou, Francis Fidelle, et al.. A single base pair duplication in SLC33A1 gene causes fetal losses and neonatal lethality in Manech Tête Rousse dairy sheep. 2023. hal-04158647

HAL Id: hal-04158647

<https://hal.inrae.fr/hal-04158647>

Preprint submitted on 11 Jul 2023

HAL is a multi-disciplinary open access archive for the deposit and dissemination of scientific research documents, whether they are published or not. The documents may come from teaching and research institutions in France or abroad, or from public or private research centers.

L'archive ouverte pluridisciplinaire **HAL**, est destinée au dépôt et à la diffusion de documents scientifiques de niveau recherche, publiés ou non, émanant des établissements d'enseignement et de recherche français ou étrangers, des laboratoires publics ou privés.

1 **A single base pair duplication in *SLC33A1* gene causes fetal**
2 **losses and neonatal lethality in Manech Tête Rouse dairy**
3 **sheep**

4 Maxime Ben Braiek¹, Soline Szymczak¹, Céline André², Philippe Bardou³, Francis Fidelle²,
5 Itsasne Granado-Tajada⁴, Florence Plisson-Petit¹, Julien Sarry¹, Florent Woloszyn¹, Carole
6 Moreno-Romieux^{1§} and Stéphane Fabre^{1*}

7 ¹GenPhySE, Université de Toulouse, INRAE, ENVT, F-31326, Castanet-Tolosan, France

8 ²CDEO, Quartier Ahetzia, 64130, Ordiarp, France

9 ³Sigenae, INRAE, 31326 Castanet-Tolosan, France

10 ⁴Department of Animal Production, NEIKER-BRTA Basque Institute of Agricultural Research
11 and Development, Agrifood Campus of Arkaute s/n, E-01080 Arkaute, Spain

12 \$ *in memoriam*

13 *Corresponding author

14 Email: stephane.fabre@inrae.fr (SF)

15 **Abstract**

16 Recently, we evidenced that the Manech Tête Rouse (MTR) deficient homozygous haplotype
17 2 (MTRDHH2) was likely to harbor a recessive lethal variant in ovine. In the present study, we
18 fine mapped this region by analyzing the whole genome sequence of five MTRDHH2
19 heterozygous carriers compared to 95 sequences of non-carrier animals from MTR and others
20 ovine breeds. We successfully identified a single base pair duplication in the *SLC33A1* gene,
21 resulting in a frameshift leading to a premature stop codon (p.Arg246Alafs*3). *SLC33A1* acts
22 as a transmembrane transporter of acetyl-Coenzyme A, essential for cellular metabolism. In

23 order to assess for the lethal phenotype in homozygous MTR sheep, we generated at-risk
24 matings by artificial insemination (AI) between rams and ewes heterozygous for the *SLC33A1*
25 variant named *SLC33A1_dupG*. Gestation status was checked 15 days post-AI by a molecular
26 test from blood expression of the interferon Tau-stimulated *MXI* gene, and by ultrasonography
27 performed between 45 days and 60 days post-AI. Based on ultrasonography, the AI success
28 was reduced by 12% compared to safe matings suggesting embryonic/fetal losses further
29 confirmed by the molecular test based on *MXI* differential expression. Forty-nine lambs were
30 born from at-risk matings with a mortality rate of 34.7% observed before weaning.
31 Homozygous *SLC33A1_dupG* lambs contributed to 47% of this mortality occurring mainly in
32 the first five days after lambing with no obvious clinical signs. Thus, an appropriate
33 management of *SLC33A1_dupG* (allele frequency of 0.04) in the MTR selection scheme should
34 increase the overall fertility and lamb survival.

35 **Keywords**

36 *Ovis aries*, homozygous haplotype deficiency, MTRDHH2, lethal variant, abortion, neonatal
37 mortality, *SLC33A1*, acetyl-CoA transporter

38 **Introduction**

39 Most individuals are expected to carry between 1 and 5 highly deleterious variants in
40 their genome known as loss-of-function alleles (Georges et al., 2019; MacArthur et al., 2012).
41 When homozygous, these variants often cause severe defects leading to lethality (from
42 embryonic stage to adulthood) or morphological disorders. The management of these defects
43 must go through the identification of the causal variants. In order to tackle this issue, recent
44 advances in the use of genomic tools have enhanced the discovery of the causative variants for
45 many genetic disorders. In human, the genome was for the first time sequenced in 2001 opening
46 up many perspectives, especially to fine-map causal variants (Lander et al., 2001). Nowadays
47 in human, 7,342 entries are reported in the OMIM database (<https://www.omim.org>, consulted
48 on 07/03/2023) for which the molecular basis is known. In livestock also, the emergence of
49 next-generation sequencing has allowed to get access to the whole genome of many individuals
50 and an exhaustive number of genetic markers as single nucleotide polymorphisms (SNP),
51 representative of the individual genome variability (Eggen, 2012; Rupp et al., 2016).
52 In order to fine-map causal variants responsible for genetic defects, two main strategies were
53 developed. The classic “top-down” strategy is based on available phenotypes and associated
54 biological samples genotyped using SNP arrays. Based on genome-wide association study with
55 a case-control approach (Uffelmann et al., 2021), and/or homozygosity mapping (Charlier et
56 al., 2008; Lander and Botstein, 1987) coupled with whole genome sequencing data, geneticists
57 can successfully fine-map causal variants. In contrast, the “bottom-up” strategy utilizes a
58 reverse genetic screen method initially developed to identify lethal variant without any available
59 phenotype (Fritz et al., 2013; VanRaden et al., 2011). This method uses high throughput SNP
60 genotyping data to detect deficit in homozygous animals leading to a significant deviation from
61 Hardy-Weinberg equilibrium is based on within trios transmission probability (VanRaden et
62 al., 2011). The establishment of routine SNP genotyping within the framework of genomic

63 selection in livestock has made possible the use this method in many species as cattle (Fritz et
64 al., 2013; VanRaden et al., 2011), beef (Jenko, 2019), pigs (Derks et al., 2017), chicken (Derks
65 et al., 2018), turkey (Abdalla et al., 2020), horses (Todd et al., 2020) and sheep (Ben Braiek et
66 al., 2023, 2021). Especially in sheep, we recently identified numerous independent deficient
67 homozygous haplotypes (DHH) in Lacaune and Manech Tête Rousse (MTR) dairy sheep (Ben
68 Braiek et al., 2023, 2021). Thanks to WGS data and generation of at-risk mating between DHH
69 heterozygous carriers, we were able to identify two nonsense variants, one in the *CCDC65* gene
70 causative of respiratory disorders leading to juvenile lethality in Lacaune (LDHH6, OMIA
71 002342-9940) (Ben Braiek et al., 2022), and another one located in the *MMUT* gene affecting
72 the propionic acid metabolism responsible for neonatal lethality in MTR (MTRDHH1) (Ben
73 Braiek et al., 2023). These two DHH were firstly associated with significant increased stillbirth
74 rate in at-risk mating based on population records. Additionally, some of the other evidenced
75 DHH (LDHH1-2-8-9 in Lacaune, and MTRDHH2 in MTR) also affected the artificial
76 insemination (AI) success by a 3% decrease in at-risk mating compared to safe mating,
77 assuming the action of lethal embryonic variants (Ben Braiek et al., 2023, 2021).

78 Embryonic and early fetal losses are difficult to observe and have strong economic impact for
79 sheep breeders (Diskin and Morris, 2008; Dixon et al., 2007). Although the causes of these
80 losses are mainly environmental, lethal genetic variants could also explain a part of this problem
81 (VanRaden et al., 2011). In sheep, fertilization failure and embryonic losses could be associated
82 with a negative gestation diagnosis realized by ultrasonography at day 45-60 post-fertilization.
83 However, most of embryonic losses are expected during the period from the fertilization (day
84 0) to the implantation of the conceptus (days 12-16) (Bindon, 1971; Spencer et al., 2008;
85 Wilmut et al., 1986). During implantation, the embryo binds to the endometrium and leads to
86 the secretion of interferon tau (IFNT) as a pregnancy recognition signal (Bazer, 2013). As a
87 response, interferon stimulated genes (ISG) expression is greatly enhanced in the endometrium

88 but also in circulating immune cells in the blood (Ott and Gifford, 2010). Among these ISG,
89 *MXI* (Myxovirus-influenza virus resistance 1), *STAT1* (Signal transducer and activator of
90 transcription 1) and *CXCL10* (Chemokine C-X-C motif ligand 10) blood expression have been
91 used to predict the gestation status at day 14-15 in sheep (Mauffré et al., 2016).

92 As presented above, the MTRDHH2 deficient haplotype in MTR dairy sheep reduced
93 significantly the AI success by 3.0%, but it also increased the stillbirth rate by 4.3%, indicating
94 a possible action of a lethal variant all along the gestation (Ben Braiek et al., 2023). MTRDHH2
95 was located on the ovine chromosome 1 (NC_040252.1, OAR1:251.9-256.4 Mb on sheep
96 genome Rambouillet_v1.0) with an estimated frequency of heterozygous carriers of 8.7%, and
97 we have reported only one functional candidate gene (*SLC33A1*) within the MTRDHH2
98 genomic region (Ben Braiek et al., 2023). The objective of this study was to evidence the causal
99 variant associated with MTRDHH2 and to validate the lethal embryonic effect by generating
100 at-risk mating and monitoring the early gestation time at day 15 by a molecular diagnosis and
101 day 45-60 by an ultrasonography diagnosis.

102 **Materials and Methods**

103 **Sequencing data, WGS variant calling and annotation**

104 The list of the 100 publicly available ovine whole genome sequences (WGS, short read Illumina
105 HiSeq/Nova Seq) coming from 14 different breeds generated in various INRAE and Teagasc
106 research projects is detailed in Table S1 (project and sample accession numbers). Among them,
107 22 WGS were from Manech Tête Rousse dairy sheep also genotyped with the Illumina
108 OvineSNP50 Beadchip in the framework of dairy sheep genomic selection program (Astruc et
109 al., 2016). They all had a known status at the MTRDHH2 haplotype encoded 0 for non-carrier
110 (n=17), 1 for heterozygous carrier (n=5) and 2 for homozygous carrier (n=0) (Ben Braiek et al.,

111 2023). Read mapping, WGS variant calling and annotation were performed using Nextflow
112 v20.10.0 and Sarek pipeline v2.6.1 as already described (Ben Braiek et al., 2023).

113 **Identification of candidate causal variants**

114 All SNPs and InDels variants located within the MTRDHH2 haplotype region extended by 1
115 Mb from each side were extracted from OAR1 (Oar_rambouillet_v1.0;
116 NC_040252.1:250,858,291-257,412,373pb) using SnpSift Filter, part of the SnpEff toolbox
117 (Cingolani et al., 2012). Correlation analysis was performed between MTRDHH2 haplotype
118 status (0, 1 and 2) and allele dosage for bi-allelic variants (also encoded 0, 1 or 2) using geno--
119 r2 command of VCFtools (Danecek et al., 2011). The putative causal variant was checked
120 manually using the Integrative Genomics Viewer (IGV) (Thorvaldsdóttir et al., 2013) using the
121 BAM files of the 22 MTR dairy sheep.

122 **Biological samples**

123 The experimental design is described in Fig. 1. Jugular blood samples from 419 MTR dairy
124 ewes (all daughters of MTRDHH2 carrier sires) located in 6 private farms were collected by a
125 habilitated veterinarian (Venoject system containing EDTA, Terumo, Tokyo, Japan) and stored
126 at -20°C either for further genotyping (n=419) or RNA extraction (n=137). Ear biopsies (1 mm³)
127 from the 49 newborn lambs were obtained with a tissue sampling unit (TSU, Allflex Europe,
128 Vitré, France) and directly placed in the TSU storage buffer at 4°C. Ear biopsies were treated
129 with consecutive action of NaOH and Tris-HCl for subsequent genotyping as previously
130 described (Ben Braiek et al., 2023).

131 DNA sets from MTR genomic lambs (n=714) with a known status at MTRDHH2 (Ben Braiek
132 et al., 2023), Manech-related Latxa Spanish sheep (n=100) and a diversity panel from 25 French
133 sheep breeds (n=749) (Rochus et al., 2018) were also used for single marker genotyping.

134 ***SLC33A1* specific genotyping assay**

135 Among the candidate variants located in MTRDHH2, a PCR allele competitive extension
136 (PACE) genotyping assay was developed for the variant NC_040252.1:g.252,649,023dupG
137 located in the *SLC33A1* gene. Fluorescent PACE analysis was done with 15ng of purified DNA
138 (from DNA panels) using the PACE-IR 2x Genotyping Master mix (3CR Bioscience) in the
139 presence of 12 μ M of a mix of extended allele specific forward primers (Table S2) in a final
140 volume of 10 μ L. The touch-down PCR amplification condition was 15 min at 94°C for the hot-
141 start activation, 10 cycles of 20s at 94°C, 54–62°C for 60s (dropping 0.8°C per cycle), then 36
142 cycles of 20s at 94°C and 60s at 54°C performed on an ABI9700 thermocycler followed by a
143 final point read of the fluorescence on an ABI QuantStudio 6 real-time PCR system and using
144 the QuantStudio software 1.3 (Applied Biosystems). For the genotyping of crude biological
145 samples (whole blood or neutralized NaOH treatment solution of ear biopsies), a preliminary
146 Terra PCR Direct Polymerase mix amplification (Takara Bio, Kusatsu, Japan) using 1 μ L of
147 crude sample was used for direct genotyping without DNA purification. The following
148 amplification primers (Table S2) were designed using Primer3Plus software (Untergasser et al.,
149 2007). This preliminary PCR was performed on an ABI2720 thermocycler (Applied
150 Biosystems, Waltham, MA, USA) with the following conditions: 5 min at 94°C, 35 cycles of
151 30s at 94°C, 30s at 58°C and 30s at 72°C, followed by 5 min final extension at 72°C. Then,
152 1 μ L of the PCR product were used for subsequent PACE genotyping.

153 **Programmed mating**

154 Among the 419 daughters of MTRDHH2 carrier sires and according to *SLC33A1* genotyping
155 results, 137 ewes were retained for programmed mating. Two groups of mating were
156 constituted: safe matings (n=73 ewes) between non-carrier ewes and rams, and at-risk matings

157 (n=64 ewes) between heterozygous-carriers. All ewes were mated by artificial insemination
158 (AI) with fresh semen. A jugular blood sample was collected from each mated ewe 15 days
159 after AI for further gestation molecular diagnosis test. An ultrasound diagnosis of gestation was
160 realized between 45 and 60 days after AI. Gestations were followed and each lamb was
161 monitored from birth to weaning age.

162 **Molecular diagnosis of gestation**

163 *RNA extraction, reverse transcription and real-time PCR*

164 Total RNAs were extracted from blood of 137 ewes with the Nucleospin® RNA Blood Kit
165 (Macherey-Nagel, #Ref 740200.50) according to the manufacturer's protocol starting with
166 800µL of whole blood with a DNaseI digestion treatment to eliminate contaminating genomic
167 DNA. RNAs was quantified by spectrophotometry (NanoDrop® ND-8000 spectrophotometer,
168 ThermoFischer) and stored at -80°C. After quality and quantity control, 91 RNA samples (n=40
169 ewes in safe mating control group and n=51 ewes in at-risk mating group) were kept for reverse
170 transcription. Reverse transcription was carried out from 500 ng of total RNA in solution with
171 anchored oligo(dT) T22V (1µL at 100µM), random oligo-dN9 (1µL at 100µM) and dNTPs
172 (2µL at 10 mM) in a reaction volume of 54µL. This mixture was incubated at 65°C for 5 min
173 in an ABI2700 thermocycler (Applied Biosystems) then ramped down to 4°C. A second
174 reaction mixture (18.5µL/reaction) containing the reaction buffer (14µL of First strand Buffer
175 5X, Invitrogen, France), DTT (Dithiothreitol, 3µL at 0.1M), Rnasine (0.5µL, 40 units/µL,
176 Promega, France) and Superscript II reverse transcriptase (1µL, 200 units/µL, Invitrogen,
177 France) was added to the denatured RNA solution (final volume reaction of 72.5µL) then
178 incubated for 50 minutes at 42°C and placed for 15 minutes at 70°C. The complementary DNA
179 (cDNA) solution obtained was directly diluted at 1:2 ratio and stored at -20°C. Quantitative
180 PCR (qPCR) was performed using 3µL of cDNA, 5µL of SYBR Green real-time PCR Master

181 Mix 2X (Applied Biosystems) and 2 μ L of primers at 3 μ M in a total reaction volume of 10 μ L.
182 Each sample was tested in quadruplicate. qPCR was realized on a QuantStudio 6 Flex Real-
183 Time PCR system (ThermoFisher). For each pair of primers, amplification efficiency was
184 evaluated by $E = e^{-1/\alpha}$ which α is the slope of a linear curve obtained from cDNA serial
185 dilution and corresponding Ct (cycle threshold) values. RNA transcript abundance was
186 quantified using the delta Ct (ΔCt) method corrected by two reference genes (*GAPDH*,
187 *YWHAZ*). Primers were design using Beacon Designer 8 (Premier Biosoft). qPCR primer
188 sequences, amplification lengths and amplification efficiencies are available in Table S2.

189 *Statistical analyses*

190 The ewe gestation status (pregnant/non-pregnant) was firstly determined by the ultrasound
191 diagnosis and thereafter corrected at the time of lambing. *MXI* and *STAT1* (Interferon
192 Stimulated Genes, ISG) relative expressions between pregnant and non-pregnant ewes were
193 compared using Wilcoxon non-parametric test.

194 The assessment of the gestation diagnosis molecular test (GDMT) at day 15 was based on the
195 ISG expression. The prediction was performed by ROC (Receiver Operating Characteristic)
196 curve analysis using easyROC (Goksuluk et al., 2016). The model was first fitted using the data
197 expression of the safe mating control group (training data) and thereafter transposed on at-risk
198 mating data expression supposed under the influence of the *SLC33AI* lethal embryonic variant
199 (testing data). For training data, the area under the curve (AUC) was evaluated and compared
200 to the expected value of 0.5 under the null hypothesis, the cut-off method ROC01 (which
201 minimizes distance between ROC curve and point (100-Sp=0, Se=100)) was used to maximize
202 Sensitivity (Se; i.e., ability of the GDMT to correctly detect pregnant ewes by ultrasonography).
203 This cut-off value was used to classified the ISG relative expression in four categories: true
204 positive (TP i.e., GDMT+ and pregnant), false positive (FP i.e., GDMT+ and non-pregnant),
205 true negative (TN i.e., GDMT- and pregnant) and false negative (FN i.e., GDMT- and non-

206 pregnant). The test estimators were generalized using the prevalence (Pr) (e.g, the probability
207 to be pregnant at day 45-60, corresponding to the population mean of 60.3% in the Manech
208 Tête Rousse overall population (Ben Braiek et al., 2023)). The positive predictive value (PPV)
209 i.e., the number of ewes with a positive GDMT and pregnant at day 45-60 among the number
210 of ewes with positive GDMT, and negative predictive value (NPV), i.e., the number of ewes
211 with a negative GDMT and non-pregnant at day 45-60 among the number of ewes with negative
212 GDMT, was determined by $PPV = \frac{Se \times Pr}{Se \times Pr + (1-Sp) \times (1-Pr)}$ and $NPV = \frac{Sp \times (1-Pr)}{Sp \times (1-Pr) + (1-Se) \times Pr}$.
213 For testing data, the cut-off value of the training model was used to classified the ewes of the
214 at-risk mating group in the TP, FP, TN and FN categories (observed numbers). The model
215 parameters (Se, Sp, Pr, PPV and NPV) were used to estimate the expected numbers in TP, FP,
216 TN and FN categories. Chi-squared tests were performed between the observed and expected
217 number of ewes with positive and negative GDMT, respectively.

218 **Results**

219 **Identification of a single base pair duplication in *SLC33A1* gene**

220 In order to identify the causative variant located in MTRDHH2 haplotype, we have scanned the
221 genome of 100 ovine WGS focusing on the polymorphisms located in MTRDHH2 region
222 extended by 1 Mb from each side (OAR1:250,858,291-257,412,373pb). In this 6.5 Mb region,
223 we detected 111,984 polymorphisms (variant call rate $\geq 95\%$, quality score > 30). Among the
224 WGS animals, 22 were from the Manech Tête Rousse breed and 5 of them were heterozygous
225 carriers of MTRDHH2. After Pearson correlation analysis between biallelic variant status
226 (SNPs and InDels) and MTRDHH2 haplotype status (all encoded by 0, 1 and 2), 189
227 polymorphisms had a perfect correlation with MTRDHH2 status (Fig. 2a). Nevertheless, only
228 one variant (NC_040252.1, OAR1:g.252,649,023dupG; Table S3) was located in a coding

229 sequence and was predicted to highly alter the *Solute carrier family 33 member 1 (SLC33A1)*
230 gene (XM_012100950.3, c.735dupG). This variant, thereafter called *SLC33A1_dupG*, is a
231 single base pair duplication of a guanine in the first exon of the gene (Fig. 2b, c). It is predicted
232 to create a premature stop codon three amino acids after the duplication (XP_011956340.1,
233 p.Arg246Alafs*3) resulting in a truncated protein of 248 amino acids compared to the 550
234 amino acids full length protein (Fig. 2d). The *SLC33A1* protein is composed of 9
235 transmembrane domains (UniProt: A0A6P3TI15_SHEEP) while in the mutant form, only 3
236 transmembrane domains can be translated.

237 **Variant association with MTRDHH2 and diversity analysis**

238 In order to validate the association of the putative causal variant located in *SLC33A1* gene with
239 *MTRDHH2*, we genotyped a DNA set from 714 Manech Tête Rousse lambs of the 2021
240 genomic cohort with a known status at *MTRDHH2* (Ben Braiek et al., 2023), and we observed
241 a variant allele frequency of 4%. The contingency table showed a strong association between
242 the OAR1: g.252,649,023dupG genotype and *MTDHH2* haplotype status (Table 1, Fischer's
243 exact test, $P < 0.0001$, without the homozygous carrier individuals). All the *MTRDHH2*
244 heterozygous carriers were also heterozygous for the *SLC33A1_dupG* variant. However, among
245 the 56 heterozygous animals for the *SLC33A1_dupG*, 14 were not *MTRDHH2* heterozygous
246 carriers. A specific focus on the 66 SNP markers composing the *MTRDHH2* haplotype showed
247 shorter recombinant versions of *MTRDHH2* (from 5 to 65 SNPs) possibly explaining this
248 discrepancy (Fig. S1).

249 **Table 1. Contingency table between MTRDHH2 status and**
 250 **NC_040252.1:g.252,649,023dupG genotype.**

Genotype	+/+	MTRDHH2/+	MTRDHH2/ MTRDHH2	Total
WT/WT	658	0	0	658
WT/dupG	14	42	0	56
dupG/dupG	0	0	0	0
Total	672	42	0	714

251 +/+ = non-carriers; MTRDHH2/+ = heterozygous carriers and MTRDHH2/MTRDHH2 = homozygous
 252 carriers (Fisher's exact test, $p < 0.001$, without the homozygous MTRDHH2 carriers).

253 In order to search for the segregation of the *SLC33A1_dupG* variant in other sheep breeds, we
 254 genotyped a DNA diversity panel of French (FR) and Spanish (ES) ovine breeds composed of
 255 28 different breeds in total. The variant was found in the heterozygous state in 3 French MTR
 256 animals and one Spanish Latxa Cara Rubia animal (Table 2).

257 **Table 2. NC_040252.1:g.252,649,023dupG genotype distribution from a DNA diversity**
 258 **panel of French (FR) and Spanish (ES) ovine breeds.**

Breed	Total	Genotype		Breed	Total	Genotype	
		WT/WT	WT/dupG			WT/WT	WT/dupG
Berrichon du Cher (FR)	30	30		Martinik (FR)	23	23	
Blanche du Massif Central (FR)	31	31		Merinos d'Arles (FR)	27	27	
Causse du Lot (FR)	32	32		Mourerous (FR)	26	26	
Charmoise (FR)	31	31		Mouton Vendéen (FR)	30	30	
Charollais (FR)	30	30		Noir du Velay (FR)	28	28	
Corse (FR)	30	30		Préalpes du sud (FR)	27	27	
Ile de France (FR)	28	28		Rava (FR)	29	29	
Lacaune (Meat) (FR)	45	45		Romane (FR)	30	30	
Lacaune (Milk) (FR)	40	40		Romanov (FR)	26	26	
Latxa Cara Negra Euskadi (ES)	30	30		Rouge de l'Ouest (FR)	30	30	
Latxa Cara Negra Navarra (ES)	40	40		Roussin (FR)	30	30	
Latxa Cara Rubia (ES)	30	29	1	Suffolk (FR)	29	29	
Limousine (FR)	29	29		Tarasconnaise (FR)	33	33	
Manech Tête Rousse (FR)	28	25	3	Texel (FR)	27	27	
				Total	849	845	4

259 ***SLC33AI_dupG* variant associated with decreased AI success and lamb**
260 **mortality**

261 MTR ewes (n=419) from 6 private farms where genotyped for the *SLC33AI_dupG* variant.
262 Among them, 137 ewes were selected to constitute two mating groups, a safe mating control
263 group with 73 non-carrier ewes mated through AI with non-carrier rams, and an at-risk mating
264 group with 64 heterozygous ewes for *SLC33AI_dupG* mated through AI with heterozygous
265 rams in order to generate *SLC33AI_dupG* homozygous lambs. Gestation was monitored by a
266 blood sampling at day 15, ultrasonography between day 45 and day 60, and lambing records at
267 151 ± 7 days after AI. As shown in Fig. 3, the AI success at ultrasonography (possibly corrected
268 by lambing results) was 60.3% in the safe mating group in line with the overall AI success in
269 the MTR population (Ben Braiek et al., 2023). However, the AI success was reduced to 48.4%
270 in the at-risk mating group of *SLC33AI_dupG* heterozygous carriers. This reduction of 12% is
271 not statistically significant ($p=0.17$) but is relevant in ovine breeding.

272 Among the 31 pregnant ewes in the at-risk mating group, 28 ewes had complete observation in
273 farm for gestation, lambing and lamb monitoring between birth and weaning at 1 month of age.
274 No abortion was observed between the time of ultrasonography (day 45-60 post-AI) and the
275 parturition. The length of the gestation ranged between 147 and 154 days in line with the MTR
276 population mean (151 ± 7 days) and 49 lambs were born and genotyped. The distribution by sex
277 and genotype is shown in Fig. 4a, and nine dupG/dupG lambs were obtained. The contingency
278 table (Table 3) between lamb genotypes and viability (alive or dead) indicated a significant
279 lower viability rate for dupG/dupG lambs (Fisher's exact test, $p\text{-value}<0.001$). The
280 *SLC33AI_dupG* homozygous lambs contributed to 47% of the mortality in at-risk matings and
281 the mortality occurred mainly in the first five days after lambing (Fig. 4b). A stillborn lamb
282 (Fig. 4c) has been expelled with the placenta at full term of gestation, and it showed
283 developmental arrest characteristic of a mid-gestation stage. Another stillborn lamb (same

284 phenotype as Fig. 4c) was obtained but no ear punch was done to genotype the animal
 285 (undermined genotype). Most of homozygous animals died between 1 and 5 days with no
 286 apparent morphological defects (Fig. 4d). Only one homozygous lamb died in the 5-30 days
 287 period and showed leg weakness and stiffness, and also spine deformity leading to locomotor
 288 problem (Fig. 4e).

289 **Table 3. Contingency table between lamb NC_040252.1:g.252,649,023dupG genotypes**
 290 **and viability.**

Viability	WT/WT	WT/dupG	dupG/dupG	-/-	Total
Alive	5	25	1	0	31
Dead	4	5	8	1	18
Total	9	30	9	1	49

291 -/-: undermined genotype due to absence of biological samples for a stillborn lamb. This animal
 292 is not taking into account for mortality rate calculation.

293 **Molecular diagnosis of gestation at day 15 to assess for fetal losses**

294 The decreased AI success in at-risk mating between *SLC33A1_dupG* heterozygous carriers
 295 suggested possible losses of homozygous embryos during the gestation period between AI and
 296 the ultrasound diagnosis at day 45-60. We then applied a gestation diagnosis molecular test
 297 (GDMT) based on blood mRNA expression levels of two interferon stimulated genes, *MXI* and
 298 *STAT1*, at day 15 as described by Mauffré et al. (Mauffré et al., 2016). RNA blood samples
 299 from 91 ewes (n=40 in safe mating group, n=51 in at-risk mating group) were analyzed by RT-
 300 qPCR (Fig. 1). The assessment of the GDMT at day 15 to predict the gestation status (pregnant
 301 /non-pregnant) at day 45-60 was performed on the safe mating control group. As shown in Fig.
 302 5a and as expected, the *MXI* relative expression in non-pregnant ewes (67.7%) was
 303 significantly increased in pregnant ewes (84.3%, p-value=0.043, Wilcoxon test). The same
 304 suggestive observation could be made for *STAT1* expression, even if the difference was not
 305 significant (p-value=0.076, Wilcoxon test). Thus, only *MXI* relative expression was retained
 306 for GDMT and reliability of the diagnostic was tested using ROC curve on data from the safe

307 mating group as training data. ROC plot showed an AUC of 0.687, differing significantly from
308 0.5 (p-value=0.033), a cut-off value (i.e., decision threshold) set at 63% and characterized by a
309 sensitivity of 75% and a specificity of 60% (Table 4, Fig. 5c and d). The prevalence (Pr) of AI
310 success was set at 60.3% (MTR population mean) and helped us to calculate the positive
311 predictive value (PPV = 74%) and the negative predictive value (NPV = 61%). The cut-off
312 value was used to classify ewes in four classes (TP, FP, TN and FN) according to GDMT (+ or
313 -) and ultrasound diagnostic at day 45-60 (Fig. 5e). Positive GDMT enabled to detect 65%
314 (TP/(TP+FP)) of pregnant ewes in the safe mating control group. In contrast, no significant
315 difference was observed for *MXI* expression between pregnant and non-pregnant ewes of the
316 at-risk mating group (p-value=0.27, Wilcoxon test, Fig. 5f). Thus, the molecular diagnostic
317 parameters (cut-off=63%, Pr=60.3%, PPV= 74% and NPV= 61%) were transposed into the
318 *MXI* expression data from at-risk mating group. In this group, the comparison of the observed
319 and expected number of ewes with a positive GDMT (*MXI* relative expression >63%) has
320 evidenced a trend to reduce the number of pregnant ewes (Chi-squared test, p=0.055) i.e. 16
321 pregnant ewes were expected with a positive GDMT while only 12 pregnant ewes were
322 observed. No significant difference was pointed out between observed and expected number of
323 pregnant ewes with a negative GDMT (Chi-squared test, p=0.44). Thus, the molecular
324 diagnosis likely evidenced fetal losses in the at-risk mating group between 15 days and 60 days
325 of gestation, with four ewes supposed to host homozygous fetuses for the *SLC33A1_dupG*
326 variant.

327 **Table 4. ROC curve analysis parameter for the gestation molecular diagnosis test based**
328 **on *MXI* mRNA level expression.**

Gene	AUC ± se	p-value	Se (%)	Sp (%)	Cut-Off (%) ¹	Pr (%)	PPV (%) ²	NPV (%) ²
<i>MXI</i>	0.687 ± 0.088	0.033	75	60	63	60.3	74	61

329 ¹ROC01 method (minimizes distance between ROC curve and point (100-Sp=0, Se=100)) was
330 used for optimal cut-off.

331 ²PPV and NPV were calculated as described in Material and Methods section taking account Se, Sp, Pr.
332 *MXI* = Myxovirus (influenza virus) resistance 1; AUC = Area under the curve; se = standard
333 error; Se = Sensitivity; Sp = Specificity; Pr = Prevalence e.g., artificial insemination success in
334 Manech Tête Rousse dairy sheep; PPV = Positive predictive value; NPV= Negative predictive
335 value.

336 **Discussion**

337 We recently reported the segregation of five MTRDHH haplotypes with deficit in
338 homozygous animals in MTR dairy sheep followed by the identification of a recessive lethal
339 variant in the *MMUT* gene carried by the MTRDHH1 haplotype increasing stillbirth rate (Ben
340 Braiek et al., 2023). In the present study, we focused on MTRDHH2, the second most
341 significant haplotype, having a negative impact on both AI success (-3.0%) and stillbirth rate
342 (+4.3%), suggesting that MTRDHH2 could also host a recessive lethal variant. Using WGS
343 data, we fine-mapped a single base pair duplication (NC_040252.1:g.252,649,023dupG) in the
344 *SLC33A1* gene previously highlighted as the only positional and functional candidate gene for
345 MTRDHH2 (Ben Braiek et al., 2023).

346 *SLC33A1* (also known as AT-1, acetyl-CoA transporter 1) is an essential protein involved
347 in metabolism for transporting acetyl-CoA through the endoplasmic reticulum (ER) membrane
348 (Jonas et al., 2010). It plays a role in N-lysine acetylation of ER proteins and regulates the
349 degradation of protein aggregates by autophagy. When *SLC33A1* is not functional, protein
350 aggregates accumulate in the ER lumen resulting in autophagic cell death (Peng et al., 2014).
351 Based on the sheep gene atlas (<http://biogps.org/sheepatlas/>; accessed 18 July 2022), *SLC33A1*
352 appeared to be ubiquitously expressed (Clark et al., 2017). In the present study, the
353 *SLC33A1_dupG* variant could result in a premature stop codon leading to a truncated protein
354 of 248 amino acids (XP_011956340.1:p.Arg246Alafs*3) compared to the full-length protein
355 encompassing 550 amino acids. Consequently, only three out of nine transmembrane domains
356 would be translated into the mutant form of ovine *SLC33A1*, resembling a natural knock-out

357 in sheep. Interestingly, *SLC33A1* is known to be embryonic lethal and decreases survival rate
358 in knock-out mouse (MGI:1332247, <http://www.informatics.jax.org>). Knockdown of *SLC33A1*
359 in zebrafish was also reported to cause defective axon outgrowth affecting BMP signaling (Liu
360 et al., 2017). Additionally, point variants in this gene were associated with congenital cataracts,
361 hearing loss, and neurodegeneration ((Huppke et al., 2012), OMIM 614482, <https://omim.org>),
362 and also autosomal dominant spastic paraplegia (Lin et al., 2008; Liu et al., 2017; Mao et al.,
363 2015); OMIM 612539) in human. These observations fit well with the decreased AI success in
364 crosses between *SLC33A1_dupG* heterozygous carriers, the increased mortality of homozygous
365 *dupG/dupG* newborn lambs, and the observation of a *dupG/dupG* lamb with locomotor problem
366 resembling spastic paraplegia. Several variants in *SLC33A1* were also associated with low
367 serum copper and ceruloplasmin in human (Huppke et al., 2012), however biochemical analyses
368 were not performed in our study.

369 The generation and birth of *SLC33A1 dupG/dupG* homozygous lambs allowed us to
370 confirm the increased stillbirth rate firstly observed for *MTRDHH2* and thus the recessive lethal
371 characteristic of this variant, heterozygous being not significantly affected. By oriented mating
372 we also observed a 12% reduction of AI success that could be associated with embryonic losses
373 in at-risk mating compared to safe mating. In order to explore this hypothesis, we tested a
374 molecular diagnosis of gestation 15 days after IA (the time of embryo implantation) to be
375 compared to the classic ultrasound test done between 45 days and 60 days post-IA. This
376 molecular test, based on expression in blood cells of the *MX1* gene, a well-known interferon-
377 tau stimulated gene (Mauffré et al., 2016), predicted 16 pregnant ewes while only 12 were really
378 pregnant. This led us to think that for 4 heterozygous ewes, fetal losses had occurred between
379 15 days and 60 days of gestation due to lethality of *dupG/dupG* homozygous fetuses. The role
380 of *SLC33A1* in regulating acetyl-CoA metabolism could largely explain embryogenesis defect.
381 Indeed, acetyl-CoA may play a major role in the regulation of cell growth, proliferation and

382 apoptosis, suggesting that metabolic deficiency in acetyl-CoA is responsible for embryo failure
383 (Tsuchiya et al., 2014).

384 Other methods of early pregnancy detection are available such as early transrectal
385 ultrasonography (Rickard et al., 2017) or circulating biomarker dosages as progesterone,
386 protein B (PSP-B) or pregnancy associated glycoproteins (PAGs) (Karen et al., 2003).
387 However, these approaches are only really effective from the 28th day of gestation after the
388 expected time of return to estrous (Mauffré et al., 2016). Even if the GDMT helped us to
389 highlight early fetal losses and offer good opportunities to predict the gestation status at day 15,
390 its application in farm is still limited today. Indeed, only 66% of the RNA samples of this study
391 were exploitable. This issue was mainly due to RNA degradation with limited storage control
392 of the blood sample when collected in farms. The samples should be frozen directly within
393 adequate buffer inactivating RNase. Focusing on the diagnosis method, the AUC of a ROC
394 curve is a good estimator for assessing the power of a diagnosis test (Janssens and Martens,
395 2020). In the present case, we get an AUC of 0.687 which is considered as acceptable (Swets,
396 1988). The cut-off value of 63% for the *MXI* relative expression was determined by the ROC01
397 method instead of the Youden index generally used in ROC analysis (Perkins and Schisterman,
398 2006). Indeed, the Youden index gives an equal weight to sensitivity and specificity, while the
399 optimal cut-off point of the ROC01 method favors the sensitivity in order to identify ewes with
400 a positive GDMT and pregnant at days 45-60. Initially, the GDMT was based on the expression
401 of two ISG, *MXI* and *STAT1*, but only *MXI* mRNA relative expression was different between
402 pregnant and non-pregnant ewes in the control group. As indicated earlier, IFNT is mainly
403 produced by the conceptus in a period between 14 to 17 days after AI and blood samples were
404 collected at day 15 as proposed in (Mauffré et al., 2016). However, *STAT1* showed a higher
405 mRNA expression at days 16-17 (Spencer et al., 2008) and the overexpression of *MXI* mRNA

406 could be maintained until day 21 in peripheral blood mononuclear cells (Yankey et al., 2001).
407 Thus, day 17 should be preferable to collect blood samples for further analysis.

408 Various variants are known in the superfamily of *SLC* genes accounting more than 400
409 members. About a hundred of *SLC* genes are associated with mendelian disorders in human
410 mainly neurometabolic diseases under an autosomal recessive mode of inheritance (Schaller
411 and Lauschke, 2019). Also in domestic animals, numerous causative variants in genes of the
412 *SLC* family were evidenced, the vast majority being in dog and cattle (see omia.org). For
413 example, and by using the reverse genetic screen approach in cattle, a missense variant in
414 *SLC35A3* gene was evidenced as responsible for CVM, the complex vertebral malformation
415 syndrome (rs438228855; (Thomsen et al., 2006; VanRaden et al., 2011)). CVM was previously
416 identified with alive homozygous calves but a huge proportion of homozygous animals died
417 during gestation. The homozygote deficient haplotype MH2 in Montbéliarde cattle was
418 associated with decreased calving rate likely caused by a nonsense variant in *SLC37A2* (p.R12*,
419 (Fritz et al., 2013)). The same *SLC37A2* gene is likely to harbor causal variants for
420 craniomandibular osteopathy in dog (Hytönen et al., 2016; Letko et al., 2020). In a rather
421 original way, alterations of the *SLC45A2* gene affected coat color in species as varied as horse
422 (Mariat et al., 2003), chicken and quail (Gunnarsson et al., 2007), medaka (Fukamachi et al.,
423 2008), tiger (Xu et al., 2013), gorilla (Prado-Martinez et al., 2013), dog (Winkler et al., 2014)
424 and cattle (Rothhammer et al., 2017). In sheep, only one variant was reported as a 1bp deletion
425 in *SLC13A1* to cause chondrodysplasia (Zhao et al., 2012). As in human, genetic screen based
426 on WGS data should allow to identify loss-of-function variants located in *SLC* family genes in
427 livestock (Charlier et al., 2016). The exploration of Ensembl variation database for sheep (a
428 dataset composed of 453 animals from 38 breeds all over the world,
429 <https://www.sheephapmap.org/>) revealed three different deleterious variants located in the
430 coding sequence of *SLC33A1*, one nonsense single nucleotide variant (SNV) segregating in

431 Composite and D'Man breeds (rs1093927723: p.Trp546*), and two missense SNV with a null
432 SIFT (sorting intolerant from tolerant) score segregating in Norduz breed (rs1089904504:
433 p.Asp172Tyr; rs1093173882: p.Tyr380Cys). These variants would likely result in loss-of-
434 function of *SLC33A1*, and further studies would be of interest to assess for an impact on
435 stillbirth rate in these breeds as observed for the *SLC33A1_dupG* we evidenced in MTR dairy
436 sheep.

437 **Conclusion**

438 Reverse genetic strategy is really effective in identifying embryonic lethal variant but also
439 hidden genetic diseases such as those affecting metabolism which can be easily confused with
440 normal lambing death due to environmental causes. The present study identified a single base
441 pair duplication in *SLC33A1* gene linked to the homozygous deficient haplotype MTRDHH2
442 previously identified in MTR dairy sheep. *SLC33A1* encodes for a transporter of acetyl-CoA,
443 essential for cellular metabolism. This could explain the impact of the mutation at different
444 moments of lamb development from fetal to perinatal stages. Anyway, with a proven role on
445 AI success and lamb mortality, an appropriate management of *SLC33A1_dupG* variant in the
446 MTR dairy sheep selection scheme should improve the overall fertility and lamb survival.

447 **Author contributions**

448 MBB performed the analyses, interpreted the results, and drafted the manuscript. SS performed
449 and analyzed the molecular diagnostic test of gestation. CA and FF managed mating in farms.
450 PB performed bioinformatics. FPP, JS and FW managed the biological samples and their
451 genotyping. MBB, CMR and SF conceived and designed the research. SF supervised the

452 analyses, helped interpret the results, wrote, reviewed and edited the final manuscript. All
453 authors read and approved the final manuscript.

454

455 **Acknowledgments**

456 We are grateful to the genotoul bioinformatics platform Toulouse Occitanie (Bioinfo Genotoul,
457 <https://doi.org/10.15454/1.5572369328961167E12>) for providing help and/or computing
458 and/or storage resources. The authors acknowledge the breeding confederations CDEO (Centre
459 Départemental de l'Élevage Ovin) and CONFELAC (Confederación de Asociaciones de
460 Criadores de Ovino de Razas Latxa y Carranzana) for providing access to private genomic data
461 and/or biological samples. We thank also the breeders involved in the project.

462

463 **Conflict of interest**

464 The authors declare no conflict of interest.

465 **Data availability statement**

466 The WGS data used in this study are publicly available, EMBL-EBI accession numbers are
467 described in Table S1.

468 **Ethic approval**

469 The experimental procedures on animals (blood sampling, ear biopsies) were approved by the
470 French Ministry of Teaching and Scientific Research and local ethical committee C2EA-115
471 (Science and Animal Health) in accordance with the European Union Directive 2010/63/EU on

472 the protection of animals used for scientific purposes (approval numbers APAFIS#30615-
473 2021032318054889 v5).

474

475 **ORCID**

476 Maxime Ben Braiek, ORCID iD <https://orcid.org/0000-0003-4770-0867>

477 Itsasne Granado–Tajada, ORCID iD <https://orcid.org/0000-0002-6557-1467>

478 Stéphane Fabre, ORCID iD <https://orcid.org/0000-0001-7350-9500>

479

480 **References**

- 481 Abdalla, E.A., Id-Lahoucine, S., Cánovas, A., Casellas, J., Schenkel, F.S., Wood, B.J., Baes,
482 C.F., 2020. Discovering lethal alleles across the turkey genome using a transmission
483 ratio distortion approach. *Anim. Genet.* 51, 876–889. <https://doi.org/10.1111/age.13003>
- 484 Astruc, J.-M., Baloché, G., Buisson, D., Labatut, J., Lagriffoul, G., Larroque, H., Robert-
485 Granie, C., Legarra, A., Barillet, F., 2016. Genomic selection in French dairy sheep.
486 *INRAE Prod. Anim.* 29, 41–55.
- 487 Bazer, F.W., 2013. Pregnancy recognition signaling mechanisms in ruminants and pigs. *J.*
488 *Anim. Sci. Biotechnol.* 4, 23. <https://doi.org/10.1186/2049-1891-4-23>
- 489 Ben Braiek, M., Fabre, S., Hozé, C., Astruc, J.-M., Moreno-Romieux, C., 2021. Identification
490 of homozygous haplotypes carrying putative recessive lethal mutations that compromise
491 fertility traits in French Lacaune dairy sheep. *Genet. Sel. Evol.* 53, 41.
492 <https://doi.org/10.1186/s12711-021-00634-1>
- 493 Ben Braiek, M., Moreno-Romieux, C., Allain, C., Bardou, P., Bordes, A., Debat, F.,
494 Drögemüller, C., Plisson-Petit, F., Portes, D., Sarry, J., Tadi, N., Woloszyn, F., Fabre,
495 S., 2022. A Nonsense Variant in CCDC65 Gene Causes Respiratory Failure Associated
496 with Increased Lamb Mortality in French Lacaune Dairy Sheep. *Genes* 13, 45.
497 <https://doi.org/10.3390/genes13010045>
- 498 Ben Braiek, M., Moreno-Romieux, C., André, C., Astruc, J.-M., Bardou, P., Bordes, A., Debat,
499 F., Fidelle, F., Hozé, C., Plisson-Petit, F., Rivemale, F., Sarry, J., Tadi, N., Woloszyn,
500 F., Fabre, S., 2023. Homozygous haplotype deficiency in Manech Tête Rouse dairy
501 sheep revealed a nonsense variant in MMUT gene affecting newborn lamb viability.
502 <https://doi.org/10.1101/2023.03.10.531894>
- 503 Bindon, B.M., 1971. Systematic Study of Preimplantation Stages of Pregnancy in the Sheep.
504 *Aust. J. Biol. Sci.* 24, 131–148. <https://doi.org/10.1071/bi9710131>
- 505 Charlier, C., Coppieters, W., Rollin, F., Desmecht, D., Agerholm, J.S., Cambisano, N., Carta,
506 E., Dardano, S., Dive, M., Fasquelle, C., Frennet, J.-C., Hanset, R., Hubin, X.,
507 Jorgensen, C., Karim, L., Kent, M., Harvey, K., Pearce, B.R., Simon, P., Tama, N., Nie,

508 H., Vandeputte, S., Lien, S., Longeri, M., Fredholm, M., Harvey, R.J., Georges, M.,
509 2008. Highly effective SNP-based association mapping and management of recessive
510 defects in livestock. *Nat. Genet.* 40, 449–454. <https://doi.org/10.1038/ng.96>
511 Charlier, C., Li, W., Harland, C., Littlejohn, M., Coppieters, W., Creagh, F., Davis, S., Druet,
512 T., Faux, P., Guillaume, F., Karim, L., Keehan, M., Kadri, N.K., Tamma, N., Spelman,
513 R., Georges, M., 2016. NGS-based reverse genetic screen for common embryonic lethal
514 mutations compromising fertility in livestock. *Genome Res.* 26, 1333–1341.
515 <https://doi.org/10.1101/gr.207076.116>
516 Cingolani, P., Patel, V.M., Coon, M., Nguyen, T., Land, S.J., Ruden, D.M., Lu, X., 2012. Using
517 *Drosophila melanogaster* as a Model for Genotoxic Chemical Mutational Studies with
518 a New Program, SnpSift. *Front. Genet.* 3, 35. <https://doi.org/10.3389/fgene.2012.00035>
519 Clark, E.L., Bush, S.J., McCulloch, M.E.B., Farquhar, I.L., Young, R., Lefevre, L., Pridans, C.,
520 Tsang, H.G., Wu, C., Afrasiabi, C., Watson, M., Whitelaw, C.B., Freeman, T.C.,
521 Summers, K.M., Archibald, A.L., Hume, D.A., 2017. A high resolution atlas of gene
522 expression in the domestic sheep (*Ovis aries*). *PLOS Genet.* 13, e1006997.
523 <https://doi.org/10.1371/journal.pgen.1006997>
524 Danecek, P., Auton, A., Abecasis, G., Albers, C.A., Banks, E., DePristo, M.A., Handsaker,
525 R.E., Lunter, G., Marth, G.T., Sherry, S.T., McVean, G., Durbin, R., 1000 Genomes
526 Project Analysis Group, 2011. The variant call format and VCFtools. *Bioinformatics*
527 27, 2156–2158. <https://doi.org/10.1093/bioinformatics/btr330>
528 Derks, M.F.L., Megens, H.-J., Bosse, M., Lopes, M.S., Harlizius, B., Groenen, M.A.M., 2017.
529 A systematic survey to identify lethal recessive variation in highly managed pig
530 populations. *BMC Genomics* 18, 858. <https://doi.org/10.1186/s12864-017-4278-1>
531 Derks, M.F.L., Megens, H.-J., Bosse, M., Visscher, J., Peeters, K., Bink, M.C.A.M., Vereijken,
532 A., Gross, C., de Ridder, D., Reinders, M.J.T., Groenen, M.A.M., 2018. A survey of
533 functional genomic variation in domesticated chickens. *Genet. Sel. Evol.* 50, 17.
534 <https://doi.org/10.1186/s12711-018-0390-1>
535 Diskin, M., Morris, D., 2008. Embryonic and Early Foetal Losses in Cattle and Other
536 Ruminants. *Reprod. Domest. Anim.* 43, 260–267. <https://doi.org/10.1111/j.1439-0531.2008.01171.x>
537
538 Dixon, A.B., Knights, M., Winkler, J.L., Marsh, D.J., Pate, J.L., Wilson, M.E., Dailey, R.A.,
539 Seidel, G., Inskeep, E.K., 2007. Patterns of late embryonic and fetal mortality and
540 association with several factors in sheep1. *J. Anim. Sci.* 85, 1274–1284.
541 <https://doi.org/10.2527/jas.2006-129>
542 Eggen, A., 2012. The development and application of genomic selection as a new breeding
543 paradigm. *Anim. Front.* 2, 10–15. <https://doi.org/10.2527/af.2011-0027>
544 Fritz, S., Capitan, A., Djari, A., Rodriguez, S.C., Barbat, A., Baur, A., Grohs, C., Weiss, B.,
545 Boussaha, M., Esquerré, D., Klopp, C., Rocha, D., Boichard, D., 2013. Detection of
546 Haplotypes Associated with Prenatal Death in Dairy Cattle and Identification of
547 Deleterious Mutations in GART, SHBG and SLC37A2. *PLoS One* 8, e65550.
548 <https://doi.org/10.1371/journal.pone.0065550>
549 Fukamachi, S., Kinoshita, M., Tsujimura, T., Shimada, A., Oda, S., Shima, A., Meyer, A.,
550 Kawamura, S., Mitani, H., 2008. Rescue From Oculocutaneous Albinism Type 4 Using
551 Medaka *slc45a2* cDNA Driven by Its Own Promoter. *Genetics* 178, 761–769.
552 <https://doi.org/10.1534/genetics.107.073387>
553 Georges, M., Charlier, C., Hayes, B., 2019. Harnessing genomic information for livestock
554 improvement. *Nat. Rev. Genet.* 20, 135–156. [https://doi.org/10.1038/s41576-018-0082-](https://doi.org/10.1038/s41576-018-0082-2)
555 2

- 556 Goksuluk, D., Korkmaz, S., Zararsiz, G., Karaagaoglu, A., Ergun, 2016. easyROC: An
557 Interactive Web-tool for ROC Curve Analysis Using R Language Environment. *R J.* 8,
558 213. <https://doi.org/10.32614/RJ-2016-042>
- 559 Gunnarsson, U., Hellström, A.R., Tixier-Boichard, M., Minvielle, F., Bed'hom, B., Ito, S.,
560 Jensen, P., Rattink, A., Vereijken, A., Andersson, L., 2007. Mutations in SLC45A2
561 Cause Plumage Color Variation in Chicken and Japanese Quail. *Genetics* 175, 867–877.
562 <https://doi.org/10.1534/genetics.106.063107>
- 563 Huppke, P., Brendel, C., Kalscheuer, V., Korenke, G.C., Marquardt, I., Freisinger, P.,
564 Christodoulou, J., Hillebrand, M., Pitelet, G., Wilson, C., Gruber-Sedlmayr, U.,
565 Ullmann, R., Haas, S., Elpeleg, O., Nürnberg, G., Nürnberg, P., Dad, S., Møller, L.B.,
566 Kaler, S.G., Gärtner, J., 2012. Mutations in SLC33A1 Cause a Lethal Autosomal-
567 Recessive Disorder with Congenital Cataracts, Hearing Loss, and Low Serum Copper
568 and Ceruloplasmin. *Am. J. Hum. Genet.* 90, 61–68.
569 <https://doi.org/10.1016/j.ajhg.2011.11.030>
- 570 Hytönen, M.K., Arumilli, M., Lappalainen, A.K., Owczarek-Lipska, M., Jagannathan, V.,
571 Hundi, S., Salmela, E., Venta, P., Sarkiala, E., Jokinen, T., Gorgas, D., Kere, J.,
572 Nieminen, P., Drögemüller, C., Lohi, H., 2016. Molecular Characterization of Three
573 Canine Models of Human Rare Bone Diseases: Caffey, van den Ende-Gupta, and Raine
574 Syndromes. *PLOS Genet.* 12, e1006037. <https://doi.org/10.1371/journal.pgen.1006037>
- 575 Janssens, A.C.J.W., Martens, F.K., 2020. Reflection on modern methods: Revisiting the area
576 under the ROC Curve. *Int. J. Epidemiol.* 49, 1397–1403.
577 <https://doi.org/10.1093/ije/dyz274>
- 578 Jenko, J., 2019. Analysis of a large dataset reveals haplotypes carrying putatively recessive
579 lethal and semi-lethal alleles with pleiotropic effects on economically important traits
580 in beef cattle 14.
- 581 Jonas, M.C., Pehar, M., Puglielli, L., 2010. AT-1 is the ER membrane acetyl-CoA transporter
582 and is essential for cell viability. *J. Cell Sci.* 123, 3378–3388.
583 <https://doi.org/10.1242/jcs.068841>
- 584 Karen, A., Beckers, J.-F., Sulon, J., de Sousa, N.M., Szabados, K., Reczigel, J., Szenci, O.,
585 2003. Early pregnancy diagnosis in sheep by progesterone and pregnancy-associated
586 glycoprotein tests. *Theriogenology* 59, 1941–1948. [https://doi.org/10.1016/S0093-691X\(02\)01289-X](https://doi.org/10.1016/S0093-691X(02)01289-X)
- 588 Lander, E.S., Botstein, D., 1987. Homozygosity Mapping: A Way to Map Human Recessive
589 Traits with the DNA of Inbred Children. *Science* 236, 1567–1570.
590 <https://doi.org/10.1126/science.2884728>
- 591 Lander, E.S., Linton, L.M., Birren, B., Nusbaum, C., Zody, M.C., Baldwin, J., Devon, K.,
592 Dewar, K., Doyle, M., FitzHugh, W., Funke, R., Gage, D., Harris, K., Heaford, A.,
593 Howland, J., Kann, L., Lehoczky, J., LeVine, R., McEwan, P., McKernan, K., Meldrim,
594 J., Mesirov, J.P., Miranda, C., Morris, W., Naylor, J., Raymond, Christina, Rosetti, M.,
595 Santos, R., Sheridan, A., Sougnez, C., Stange-Thomann, N., Stojanovic, N.,
596 Subramanian, A., Wyman, D., Rogers, J., Sulston, J., Ainscough, R., Beck, S., Bentley,
597 D., Burton, J., Clee, C., Carter, N., Coulson, A., Deadman, R., Deloukas, P., Dunham,
598 A., Dunham, I., Durbin, R., French, L., Grafham, D., Gregory, S., Hubbard, T.,
599 Humphray, S., Hunt, A., Jones, M., Lloyd, C., McMurray, A., Matthews, L., Mercer,
600 S., Milne, S., Mullikin, J.C., Mungall, A., Plumb, R., Ross, M., Shownkeen, R., Sims,
601 S., Waterston, R.H., Wilson, R.K., Hillier, L.W., McPherson, J.D., Marra, M.A.,
602 Mardis, E.R., Fulton, L.A., Chinwalla, A.T., Pepin, K.H., Gish, W.R., Chissole, S.L.,
603 Wendl, M.C., Delehaunty, K.D., Miner, T.L., Delehaunty, A., Kramer, J.B., Cook, L.L.,
604 Fulton, R.S., Johnson, D.L., Minx, P.J., Clifton, S.W., Hawkins, T., Branscomb, E.,
605 Predki, P., Richardson, P., Wenning, S., Slezak, T., Doggett, N., Cheng, J.-F., Olsen,

606 A., Lucas, S., Elkin, C., Uberbacher, E., Frazier, M., Gibbs, R.A., Muzny, D.M.,
607 Scherer, S.E., Bouck, J.B., Sodergren, E.J., Worley, K.C., Rives, C.M., Gorrell, J.H.,
608 Metzker, M.L., Naylor, S.L., Kucherlapati, R.S., Nelson, D.L., Weinstock, G.M.,
609 Sakaki, Y., Fujiyama, A., Hattori, M., Yada, T., Toyoda, A., Itoh, T., Kawagoe, C.,
610 Watanabe, H., Totoki, Y., Taylor, T., Weissenbach, J., Heilig, R., Saurin, W.,
611 Artiguenave, F., Brottier, P., Bruls, T., Pelletier, E., Robert, C., Wincker, P., Rosenthal,
612 A., Platzer, M., Nyakatura, G., Taudien, S., Rump, A., Smith, D.R., Doucette-Stamm,
613 L., Rubenfield, M., Weinstock, K., Lee, H.M., Dubois, J., Yang, H., Yu, J., Wang, J.,
614 Huang, G., Gu, J., Hood, L., Rowen, L., Madan, A., Qin, S., Davis, R.W., Federspiel,
615 N.A., Abola, A.P., Proctor, M.J., Roe, B.A., Chen, F., Pan, H., Ramser, J., Lehrach, H.,
616 Reinhardt, R., McCombie, W.R., de la Bastide, M., Dedhia, N., Blöcker, H., Hornischer,
617 K., Nordsiek, G., Agarwala, R., Aravind, L., Bailey, J.A., Bateman, A., Batzoglu, S.,
618 Birney, E., Bork, P., Brown, D.G., Burge, C.B., Cerutti, L., Chen, H.-C., Church, D.,
619 Clamp, M., Copley, R.R., Doerks, T., Eddy, S.R., Eichler, E.E., Furey, T.S., Galagan,
620 J., Gilbert, J.G.R., Harmon, C., Hayashizaki, Y., Haussler, D., Hermjakob, H., Hokamp,
621 K., Jang, W., Johnson, L.S., Jones, T.A., Kasif, S., Kasprzyk, A., Kennedy, S., Kent,
622 W.J., Kitts, P., Koonin, E.V., Korf, I., Kulp, D., Lancet, D., Lowe, T.M., McLysaght,
623 A., Mikkelsen, T., Moran, J.V., Mulder, N., Pollara, V.J., Ponting, C.P., Schuler, G.,
624 Schultz, J., Slater, G., Smit, A.F.A., Stupka, E., Szustakowki, J., Thierry-Mieg, D.,
625 Thierry-Mieg, J., Wagner, L., Wallis, J., Wheeler, R., Williams, A., Wolf, Y.I., Wolfe,
626 K.H., Yang, S.-P., Yeh, R.-F., Collins, F., Guyer, M.S., Peterson, J., Felsenfeld, A.,
627 Wetterstrand, K.A., Myers, R.M., Schmutz, J., Dickson, M., Grimwood, J., Cox, D.R.,
628 Olson, M.V., Kaul, R., Raymond, Christopher, Shimizu, N., Kawasaki, K., Minoshima,
629 S., Evans, G.A., Athanasiou, M., Schultz, R., Patrinos, A., Morgan, M.J., International
630 Human Genome Sequencing Consortium, Whitehead Institute for Biomedical Research,
631 C. for G.R., The Sanger Centre:, Washington University Genome Sequencing Center,
632 US DOE Joint Genome Institute:, Baylor College of Medicine Human Genome
633 Sequencing Center:, RIKEN Genomic Sciences Center:, Genoscope and CNRS UMR-
634 8030:, Department of Genome Analysis, I. of M.B., GTC Sequencing Center:, Beijing
635 Genomics Institute/Human Genome Center:, Multimegabase Sequencing Center, T.I.
636 for S.B., Stanford Genome Technology Center:, University of Oklahoma's Advanced
637 Center for Genome Technology:, Max Planck Institute for Molecular Genetics:, Cold
638 Spring Harbor Laboratory, L.A.H.G.C., GBF—German Research Centre for
639 Biotechnology:, *Genome Analysis Group (listed in alphabetical order, also includes
640 individuals listed under other headings):, Scientific management: National Human
641 Genome Research Institute, U.N.I. of H., Stanford Human Genome Center:, University
642 of Washington Genome Center:, Department of Molecular Biology, K.U.S. of M.,
643 University of Texas Southwestern Medical Center at Dallas:, Office of Science, U.D. of
644 E., The Wellcome Trust:, 2001. Initial sequencing and analysis of the human genome.
645 *Nature* 409, 860–921. <https://doi.org/10.1038/35057062>
646 Letko, A., Leuthard, F., Jagannathan, V., Corlazzoli, D., Matiasek, K., Schweizer, D., Hytönen,
647 M.K., Lohi, H., Leeb, T., Drögemüller, C., 2020. Whole Genome Sequencing Indicates
648 Heterogeneity of Hyperostotic Disorders in Dogs. *Genes* 11, 163.
649 <https://doi.org/10.3390/genes11020163>
650 Lin, P., Li, Jianwei, Liu, Q., Mao, F., Li, Jisheng, Qiu, R., Hu, H., Song, Y., Yang, Y., Gao, G.,
651 Yan, C., Yang, W., Shao, C., Gong, Y., 2008. A Missense Mutation in SLC33A1, which
652 Encodes the Acetyl-CoA Transporter, Causes Autosomal-Dominant Spastic Paraplegia
653 (SPG42). *Am. J. Hum. Genet.* 83, 752–759. <https://doi.org/10.1016/j.ajhg.2008.11.003>

654 Liu, P., Jiang, B., Ma, J., Lin, P., Zhang, Y., Shao, C., Sun, W., Gong, Y., 2017. S113R mutation
655 in SLC33A1 leads to neurodegeneration and augmented BMP signaling in a mouse
656 model. *Dis. Model. Mech.* 10, 53–62. <https://doi.org/10.1242/dmm.026880>

657 MacArthur, D.G., Balasubramanian, S., Frankish, A., Huang, N., Morris, J., Walter, K., Jostins,
658 L., Habegger, L., Pickrell, J.K., Montgomery, S.B., Albers, C.A., Zhang, Z.D., Conrad,
659 D.F., Lunter, G., Zheng, H., Ayub, Q., DePristo, M.A., Banks, E., Hu, M., Handsaker,
660 R.E., Rosenfeld, J.A., Fromer, M., Jin, M., Mu, X.J., Khurana, E., Ye, K., Kay, M.,
661 Saunders, G.I., Suner, M.-M., Hunt, T., Barnes, I.H.A., Amid, C., Carvalho-Silva, D.R.,
662 Bignell, A.H., Snow, C., Yngvadottir, B., Bumpstead, S., Cooper, D.N., Xue, Y.,
663 Romero, I.G., Consortium, 1000 Genomes Project, Wang, J., Li, Y., Gibbs, R.A.,
664 McCarroll, S.A., Dermitzakis, E.T., Pritchard, J.K., Barrett, J.C., Harrow, J., Hurles,
665 M.E., Gerstein, M.B., Tyler-Smith, C., 2012. A Systematic Survey of Loss-of-Function
666 Variants in Human Protein-Coding Genes. *Science* 335, 823–828.
667 <https://doi.org/10.1126/science.1215040>

668 Mao, F., Li, Z., Zhao, B., Lin, P., Liu, P., Zhai, M., Liu, Q., Shao, C., Sun, W., Gong, Y., 2015.
669 Identification and Functional Analysis of a SLC33A1: c.339T>G (p.Ser113Arg) Variant
670 in the Original SPG42 Family. *Hum. Mutat.* 36, 240–249.
671 <https://doi.org/10.1002/humu.22732>

672 Mariat, D., Taourit, S., Guérin, G., 2003. A mutation in the MATP gene causes the cream coat
673 colour in the horse. *Genet. Sel. Evol.* 35, 119. <https://doi.org/10.1186/1297-9686-35-1-119>

675 Mauffré, V., Grimard, B., Eozenou, C., Inghels, S., Silva, L., Giraud-Delville, C., Capo, D.,
676 Sandra, O., Constant, F., 2016. Interferon stimulated genes as peripheral diagnostic
677 markers of early pregnancy in sheep: a critical assessment. *Animal* 10, 1856–1863.
678 <https://doi.org/10.1017/S175173111600077X>

679 Ott, T.L., Gifford, C.A., 2010. Effects of Early Conceptus Signals on Circulating Immune Cells:
680 Lessons from Domestic Ruminants. *Am. J. Reprod. Immunol.* 64, 245–254.
681 <https://doi.org/10.1111/j.1600-0897.2010.00912.x>

682 Peng, Y., Li, M., Clarkson, B.D., Pehar, M., Lao, P.J., Hillmer, A.T., Barnhart, T.E., Christian,
683 B.T., Mitchell, H.A., Bendlin, B.B., Sandor, M., Puglielli, L., 2014. Deficient Import of
684 Acetyl-CoA into the ER Lumen Causes Neurodegeneration and Propensity to
685 Infections, Inflammation, and Cancer. *J. Neurosci.* 34, 6772–6789.
686 <https://doi.org/10.1523/JNEUROSCI.0077-14.2014>

687 Perkins, N.J., Schisterman, E.F., 2006. The Inconsistency of “Optimal” Cut-points Using Two
688 ROC Based Criteria. 11.

689 Prado-Martinez, J., Hernando-Herraez, I., Lorente-Galdos, B., Dabad, M., Ramirez, O., Baeza-
690 Delgado, C., Morcillo-Suarez, C., Alkan, C., Hormozdiari, F., Raineri, E., Estellé, J.,
691 Fernandez-Callejo, M., Valles, M., Ritscher, L., Schöneberg, T., de la Calle-Mustienes,
692 E., Casillas, S., Rubio-Acero, R., Melé, M., Engelken, J., Caceres, M., Gomez-
693 Skarmeta, J.L., Gut, M., Bertranpetit, J., Gut, I.G., Abello, T., Eichler, E.E., Mingarro,
694 I., Lalueza-Fox, C., Navarro, A., Marques-Bonet, T., 2013. The genome sequencing of
695 an albino Western lowland gorilla reveals inbreeding in the wild. *BMC Genomics* 14,
696 363. <https://doi.org/10.1186/1471-2164-14-363>

697 Rickard, J.P., Ryan, G., Hall, E., de Graaf, S.P., Hermes, R., 2017. Using transrectal ultrasound
698 to examine the effect of exogenous progesterone on early embryonic loss in sheep.
699 *PLOS ONE* 12, e0183659. <https://doi.org/10.1371/journal.pone.0183659>

700 Rochus, C.M., Tortereau, F., Plisson-Petit, F., Restoux, G., Moreno-Romieux, C., Tossier-
701 Klopp, G., Servin, B., 2018. Revealing the selection history of adaptive loci using
702 genome-wide scans for selection: an example from domestic sheep. *BMC Genomics* 19,
703 71. <https://doi.org/10.1186/s12864-018-4447-x>

704 Rothhammer, S., Kunz, E., Seichter, D., Krebs, S., Wassertheurer, M., Fries, R., Brem, G.,
705 Medugorac, I., 2017. Detection of two non-synonymous SNPs in SLC45A2 on BTA20
706 as candidate causal mutations for oculocutaneous albinism in Braunvieh cattle. *Genet.*
707 *Sel. Evol.* 49, 73. <https://doi.org/10.1186/s12711-017-0349-7>

708 Rupp, R., Mucha, S., Larroque, H., McEwan, J., Conington, J., 2016. Genomic application in
709 sheep and goat breeding. *Anim. Front.* 6, 39–44. <https://doi.org/10.2527/af.2016-0006>

710 Schaller, L., Lauschke, V.M., 2019. The genetic landscape of the human solute carrier (SLC)
711 transporter superfamily. *Hum. Genet.* 138, 1359–1377. <https://doi.org/10.1007/s00439-019-02081-x>

712

713 Spencer, T.E., Sandra, O., Wolf, E., 2008. Genes involved in conceptus–endometrial
714 interactions in ruminants: insights from reductionism and thoughts on holistic
715 approaches. *Reproduction* 135, 165–179. <https://doi.org/10.1530/REP-07-0327>

716 Swets, J.A., 1988. Measuring the Accuracy of Diagnostic Systems. *Science* 240, 1285–1293.
717 <https://doi.org/10.1126/science.3287615>

718 Thomsen, B., Horn, P., Panitz, F., Bendixen, E., Petersen, A.H., Holm, L.-E., Nielsen, V.H.,
719 Agerholm, J.S., Arnbjerg, J., Bendixen, C., 2006. A missense mutation in the bovine
720 SLC35A3 gene, encoding a UDP-N-acetylglucosamine transporter, causes complex
721 vertebral malformation. *Genome Res.* 16, 97–105. <https://doi.org/10.1101/gr.3690506>

722 Thorvaldsdóttir, H., Robinson, J.T., Mesirov, J.P., 2013. Integrative Genomics Viewer (IGV):
723 high-performance genomics data visualization and exploration. *Brief. Bioinform.* 14,
724 178–192. <https://doi.org/10.1093/bib/bbs017>

725 Todd, E.T., Thomson, P.C., Hamilton, N.A., Ang, R.A., Lindgren, G., Viklund, Å., Eriksson,
726 S., Mikko, S., Strand, E., Velie, B.D., 2020. A genome-wide scan for candidate lethal
727 variants in Thoroughbred horses. *Sci. Rep.* 10, 13153. <https://doi.org/10.1038/s41598-020-68946-8>

728

729 Tsuchiya, Y., Pham, U., Hu, W., Ohnuma, S., Gout, I., 2014. Changes in Acetyl CoA Levels
730 during the Early Embryonic Development of *Xenopus laevis*. *PLOS ONE* 9, e97693.
731 <https://doi.org/10.1371/journal.pone.0097693>

732 Uffelmann, E., Huang, Q.Q., Munung, N.S., de Vries, J., Okada, Y., Martin, A.R., Martin, H.C.,
733 Lappalainen, T., Posthuma, D., 2021. Genome-wide association studies. *Nat. Rev.*
734 *Methods Primer* 1, 1–21. <https://doi.org/10.1038/s43586-021-00056-9>

735 Untergasser, A., Nijveen, H., Rao, X., Bisseling, T., Geurts, R., Leunissen, J.A.M., 2007.
736 Primer3Plus, an enhanced web interface to Primer3. *Nucleic Acids Res.* 35, W71–W74.
737 <https://doi.org/10.1093/nar/gkm306>

738 VanRaden, P.M., Olson, K.M., Null, D.J., Hutchison, J.L., 2011. Harmful recessive effects on
739 fertility detected by absence of homozygous haplotypes. *J. Dairy Sci.* 94, 6153–6161.
740 <https://doi.org/10.3168/jds.2011-4624>

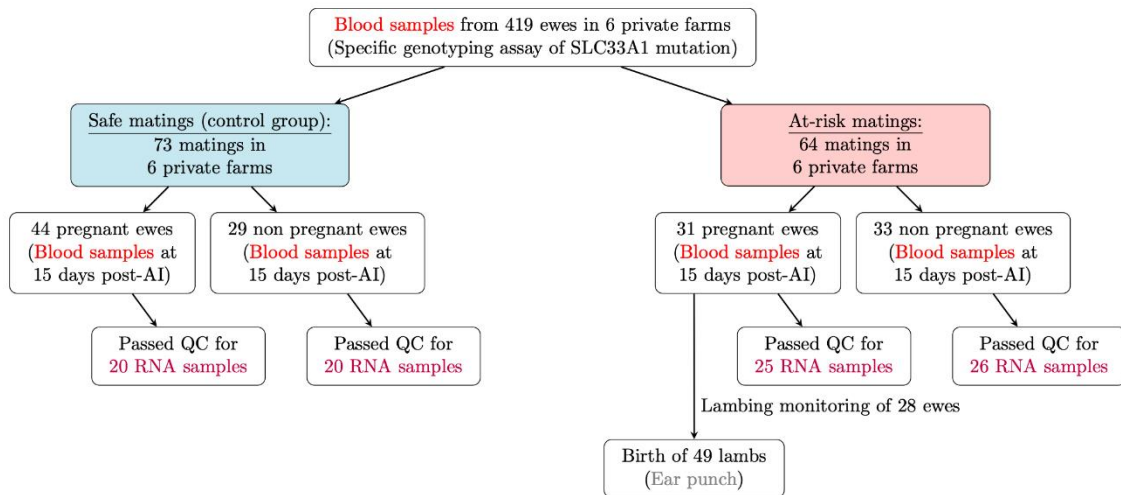
741 Wilmut, I., Sales, D.I., Ashworth, C.J., 1986. Maternal and embryonic factors associated with
742 prenatal loss in mammals. *Reproduction* 76, 851–864.
743 <https://doi.org/10.1530/jrf.0.0760851>

744 Winkler, P.A., Gornik, K.R., Ramsey, D.T., Dubielzig, R.R., Venta, P.J., Petersen-Jones, S.M.,
745 Bartoe, J.T., 2014. A Partial Gene Deletion of SLC45A2 Causes Oculocutaneous
746 Albinism in Doberman Pinscher Dogs. *PLOS ONE* 9, e92127.
747 <https://doi.org/10.1371/journal.pone.0092127>

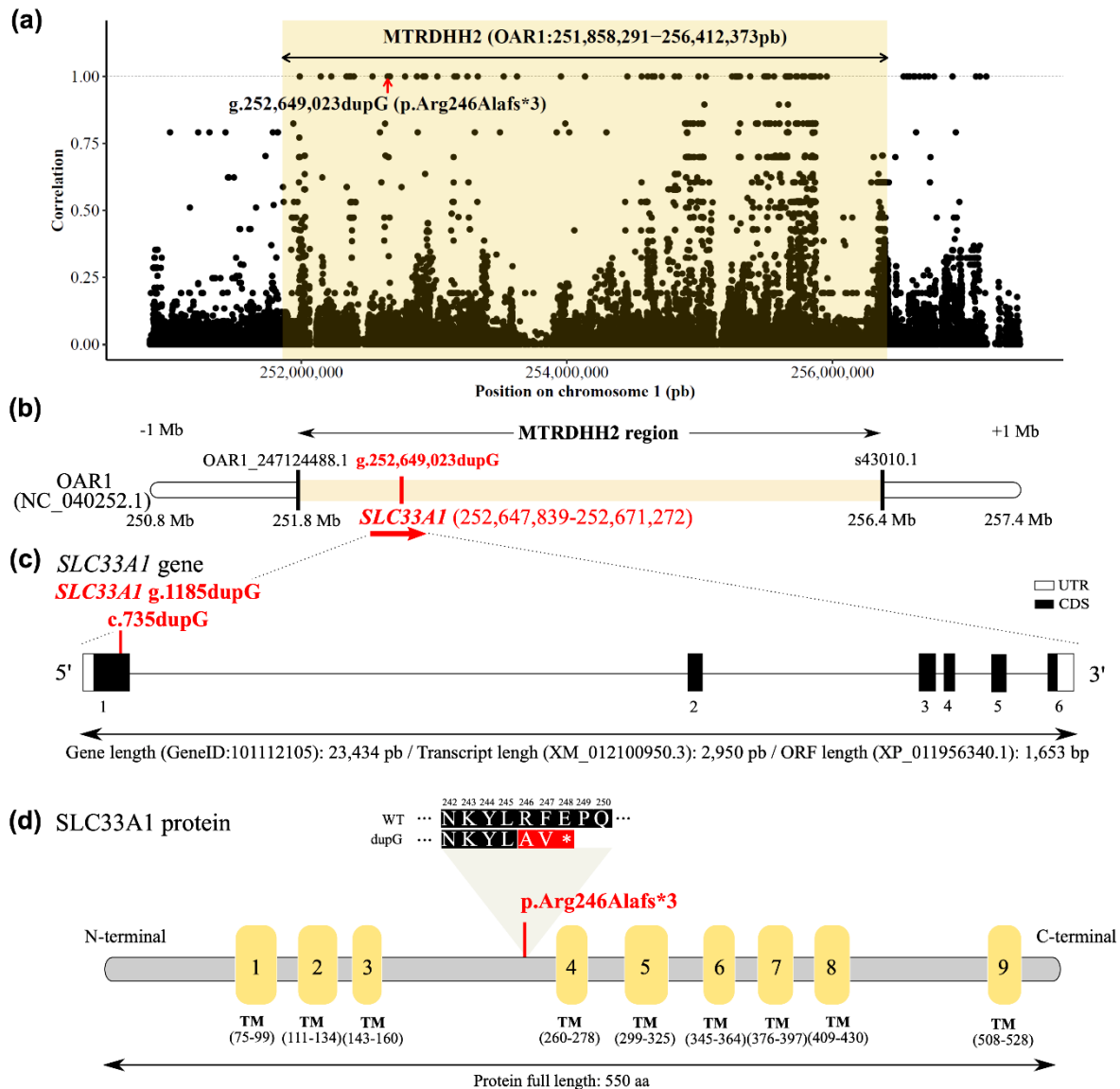
748 Xu, X., Dong, G.-X., Hu, X.-S., Miao, L., Zhang, X.-L., Zhang, D.-L., Yang, H.-D., Zhang, T.-
749 Y., Zou, Z.-T., Zhang, T.-T., Zhuang, Y., Bhak, J., Cho, Y.S., Dai, W.-T., Jiang, T.-J.,
750 Xie, C., Li, R., Luo, S.-J., 2013. The Genetic Basis of White Tigers. *Curr. Biol.* 23,
751 1031–1035. <https://doi.org/10.1016/j.cub.2013.04.054>

752 Yankey, S.J., Hicks, B.A., Carnahan, K.G., Assiri, A.M., Sinor, S.J., Kodali, K., Stellflug, J.N.,
753 Ott, T.L., 2001. Expression of the antiviral protein Mx in peripheral blood mononuclear

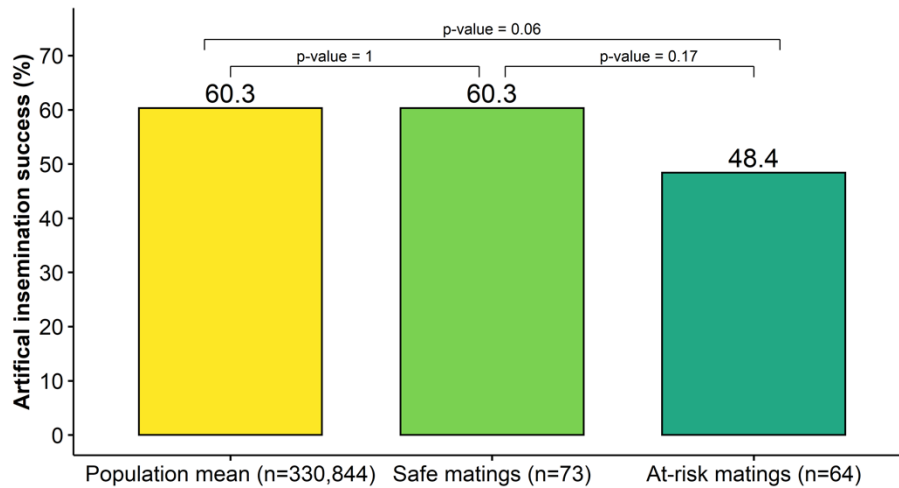
754 cells of pregnant and bred, non-pregnant ewes. *J. Endocrinol.* 170, R7-11.
755 <https://doi.org/10.1677/joe.0.170r007>
756 Zhao, X., Onteru, S.K., Piripi, S., Thompson, K.G., Blair, H.T., Garrick, D.J., Rothschild, M.F.,
757 2012. In a shake of a lamb's tail: using genomics to unravel a cause of chondrodysplasia
758 in Texel sheep. *Anim. Genet.* 43, 9–18. [https://doi.org/10.1111/j.1365-](https://doi.org/10.1111/j.1365-2052.2011.02304.x)
759 [2052.2011.02304.x](https://doi.org/10.1111/j.1365-2052.2011.02304.x)



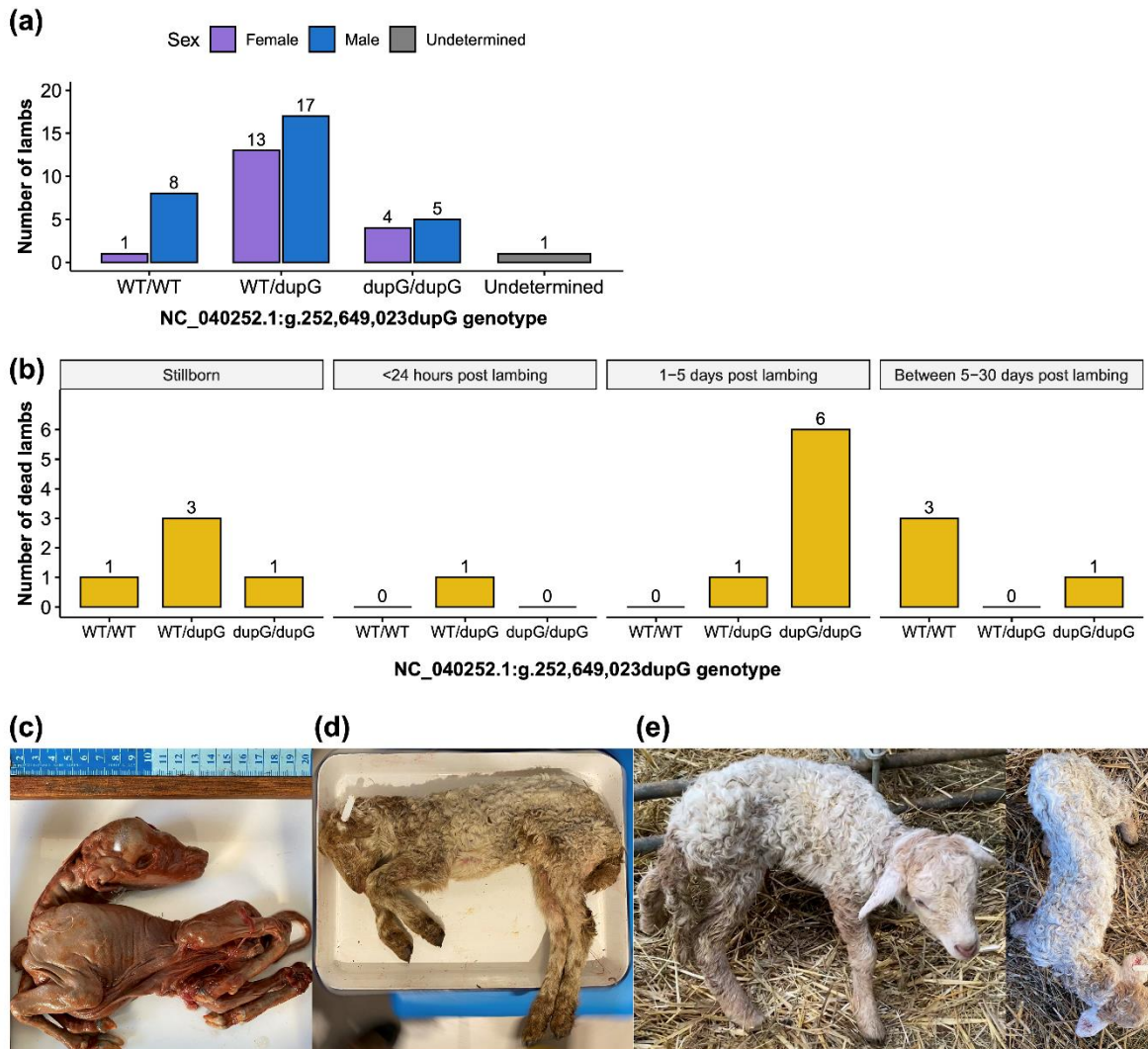
761 **Figure 1. Experimental design.** Two groups of ewes (safe matings n=73 and at-risk matings
 762 n=64) were artificially inseminated with ram fresh semen. Safe mating refers to mating between
 763 non-carrier ewes and rams. At-risk mating refers to mating between heterozygous carrier ewes
 764 and rams. QC= quality and quantity control.



765 **Figure 2. Identification of a single base pair duplication in *SLC33A1* gene.** (a) Scatter plot
 766 of the correlation between MTRDHH2 status (NC_040252.1, OAR1:251,858,291-
 767 256,412,373pb extended from each side by 1 Mb) and genotype of variants from 100 whole
 768 genome sequenced animals. Each dot represents one variant. (b) Position of the *SLC33A1* gene
 769 within the MTRDHH2 haplotype. Black bars indicate the first and the last markers of the
 770 Illumina Ovine SNP50 BeadChip defining the limits of MTRDHH2 (Ben Braiek et al., 2023).
 771 (c) *SLC33A1* gene structure (GeneID: 101112105) and localization of the c.735dupG variant
 772 identified in the first exon (XM_012100950.3). (UTR: untranslated region; CDS: coding
 773 sequence) (d) *SLC33A1* protein (XP_011956340.1) with UniProt domain annotations
 774 (accession number: A0A6P3TI15_SHEEP) composed of 9 transmembrane domains (TM). The
 775 single base pair duplication creates a premature stop codon at amino-acid position 248.

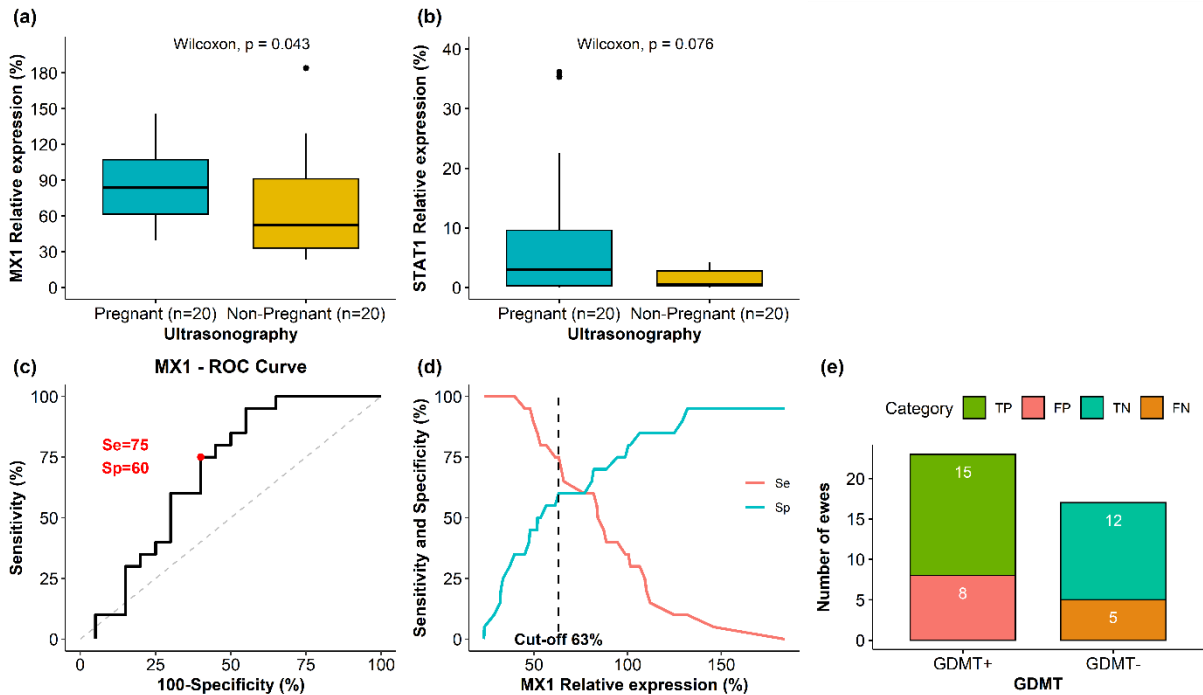


776 **Figure 3. Artificial insemination success in MTR.** MTR population artificial insemination
 777 (AI) success is based on lambing date according to the gestation length starting from the day of
 778 AI (151 ± 7 days) and was established using populational matings records (n=330,844; Ben
 779 Braiek et al., 2023). Safe and at-risk matings between *SLC33AI_dupG* carriers were realized in
 780 6 private farms (n=137 ewes) with a gestation diagnosis realized by ultrasonography between
 781 days 45 and 60. In these experimental groups, AI success could have been corrected by lambing
 782 record. AI success could have been corrected by lambing record. P-values were obtained by
 783 Fisher's exact test.

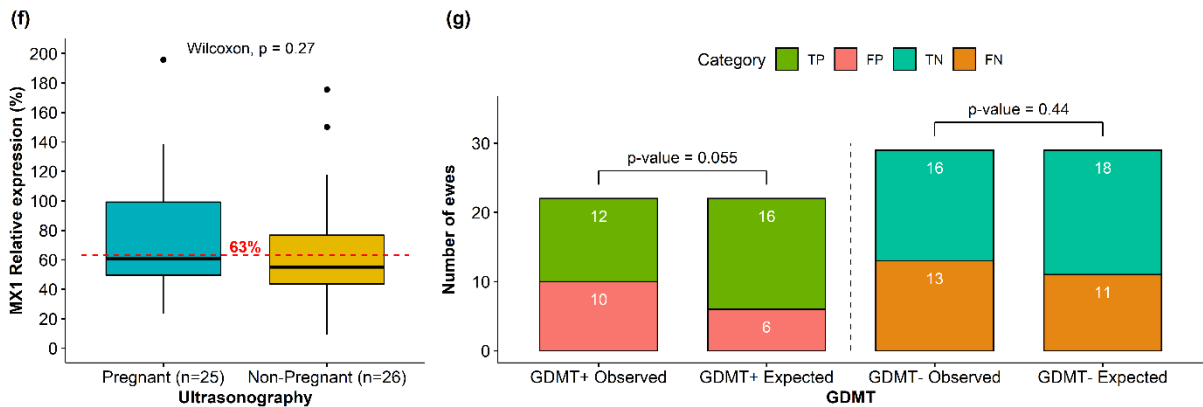


784 **Figure 4. Lambing record from at-risk matings.** (a) Distribution of the 49 lambs obtained
 785 from 28 pregnant ewes according to the *SLC33A1_dupG* genotype (one stillborn lamb not
 786 genotyped). (b) Time distribution of 17 dead lambs in the pre-weaning period with bar charts
 787 depending on *SLC33A1_dupG* genotype. (c) Stillborn lamb. (d) Dead lamb in the first 5 days
 788 post-lambing (1.750kg). (e) Alive lamb after 5 days post-lambing (dead before weaning) with
 789 morphologic and locomotor defects.

Safe Matings (Control group)



At-risk Matings



790 **Figure 5. Gestation diagnosis molecular test (GDMT).** Relative expression at 15 days post-
 791 IA of *MX1* (a) and *STAT1* (b) mRNA in pregnant and non-pregnant ewes assessed by
 792 ultrasonography in safe matings as control group. (c) ROC curve based on sensitivity (Se) and
 793 specificity (Sp) of GDMT using *MX1* relative expression in the control group. (d)
 794 Determination of *MX1* relative expression cut-off value (63%) associated with $Se=75\%$ and
 795 $Sp=60\%$ in the control group using the ROC01 method. (e) Distribution of pregnant and non-
 796 pregnant ewes according to GDMT based on *MX1* relative expression in the control group (TP,
 797 true positive; FP, false positive; TN, true negative; FN, false negative). (f) *MX1* relative
 798 expression between pregnant and non-pregnant ewes in at-risk matings. (g) Distribution of
 799 observed and expected pregnant and non-pregnant ewes according to GDMT based on *MX1*
 800 relative expression with a cut-off value of 63% in at-risk matings. The expected numbers were
 801 calculated based on prevalence ($Pr = 60.3\%$), positive predictive value ($PPV = 74\%$) and
 802 negative predictive value ($NPV = 61\%$). Differences between observed and expected numbers
 803 from GDMT (+ and -) were assessed by a Chi-squared test.

804 **Supporting information**

805 **Table S1. EMBL-EBI accession numbers of the 100 whole-genome sequences used in the**
806 **analysis.**

807 **Table S2. List of PCR primer sequences.**

808 **Table S3. List of variants located in MTRDHH2 extended by 1 Mb from each side with**
809 **perfect correlation with MTRDHH2 status.**

810 **Figure S1. MTRDHH2 recombinant haplotypes from 14 animals showing mismatch**
811 **between MTRDHH2 status and *SLC33A1_dupG* genotype.** MTRDHH2/+ and +/+ refer to
812 heterozygous and non-carriers of MTRDHH2, respectively. The grey column represents the
813 localization of *SLC33A1_dupG* (g.252,649,023dupG) within the MTRDHH2 haplotype. For
814 each animal, only the phase supposed to host the *SLC33A1_dupG* is represented. The blue color
815 indicates the portion of local haplotype matching with the MTRDHH2 haplotype.